

Interannual climate variations in Arctic as driven by the Global atmosphere oscillation



E-mail: iserykh@ocean.ru

Serykh I.V., Byshev V.I., Neiman V.G., Sidorova A.N., Sonechkin D.M.

P.P. Shirshov Institute of Oceanology, Russian Academy of Sciences

The present-day global climate change affects the Arctic basin most notably because of the sea ice cover extinction and the permafrost melting. But there are substantial variations of these effects from year to year. We believe the variance might be a regional manifestation of the planetary-scale phenomenon named as Global atmospheric oscillation (GAO). GAO [Byshev et al., 2012] includes the following well-known El Niño - Southern Oscillation (ENSO) events as well as similar processes in equatorial Atlantic and Indian Ocean, and so on. In this report we intended to present some new arguments in support the climatic GAO factor hypothesis. For this goal it was considered some interrelations between the above-mentioned Arctic anomalies and GAO as it could be seen in the global re-analyses of the sea level pressure (SLP) and near surface temperature (NST) for the period of 1920-2013. The mean global fields of SLP and NST have been computed in the time binding to all El Niño events falling into this time period, and separately, for all La Niña events. A vector difference of the fields was interpreted as amplitude of temperature-pressure anomalies forced by the Global Atmospheric Oscillation. Statistical significance of the non-zero values of the resulting fields, i.e. the reality of GAO, was evaluated with the t-Student's test. It turned out that the main spatial structures of GAO, presented specifically by El Niño and La Niña events in Pacific region, exist at a very high level (up to 99%, $t > 4$) of the significance. Therefore, one can conclude that the interannual-scale dynamics of GAO is actually reflected in the climate features of different regions of the Earth, including Arctic area. In particular, when an El Niño phase of GAO falls on the boreal winter it is indicative by a negative anomaly of NST (about -1°C) and a positive anomaly of SLP over the Arctic basin. In contrary, significant (about $+1^\circ\text{C}$) positive anomaly of NST along with reduced SLP over the whole Arctic region is typical timing with any La Niña event (up to 95%, $t > 2$).

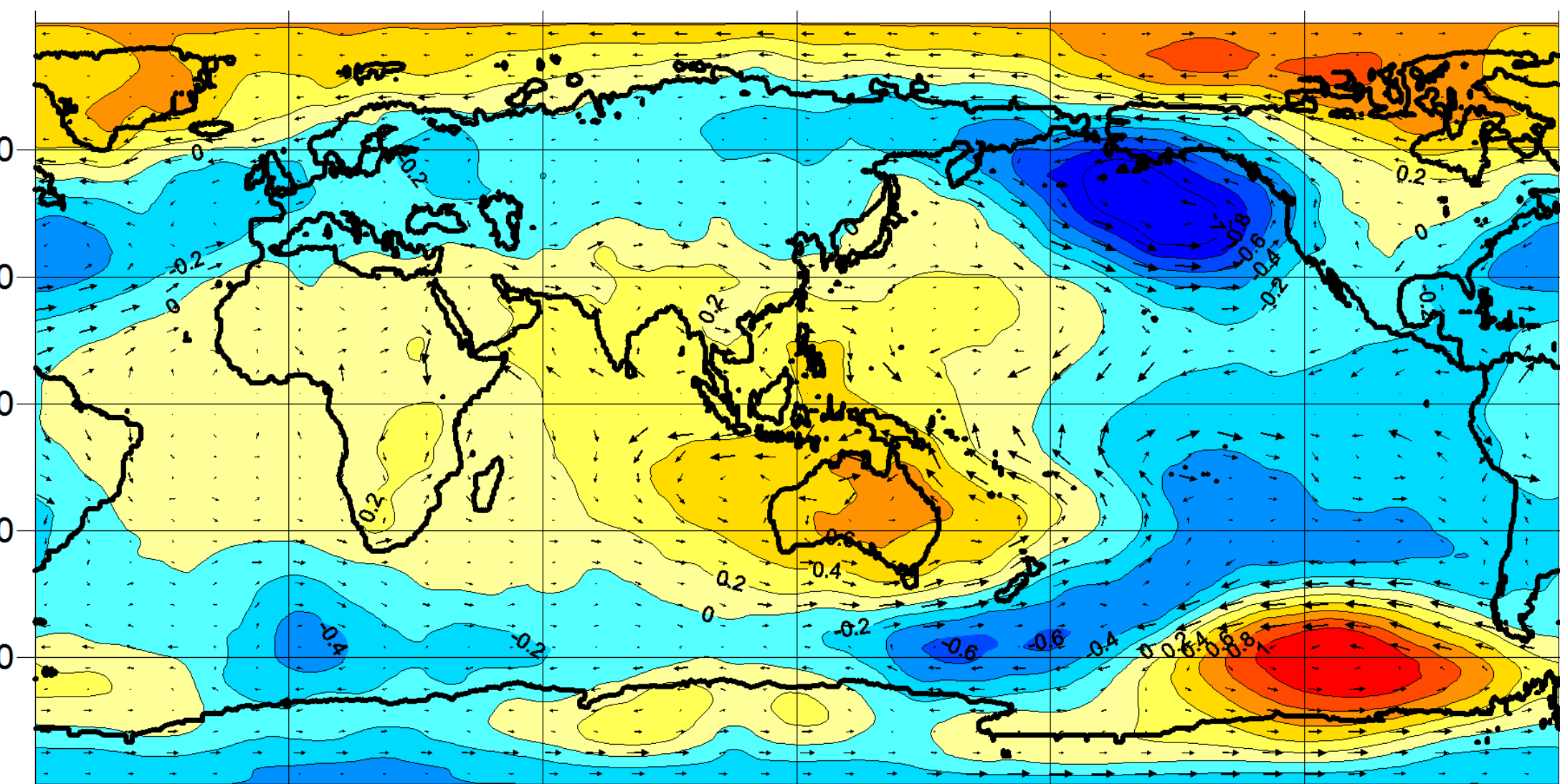
To control the reliability of GAO, numerical modeling of the hydrophysical variability of the Barents Sea was carried out for the period of the strongest El Niño event during 1997-98. A complex analysis of the modeling results corroborated that during the El Niño phase of GAO the following phenomena took place:

- the shortage of the transportation of relatively warm and saline North-Atlantic water along with intensification of the encounter water flow of the Polar origin;
- a strengthening of vertical convection along with a lowering of overall heat content of sea water column;
- a weakening of the water dynamic in the system of the general cyclonic gyre.

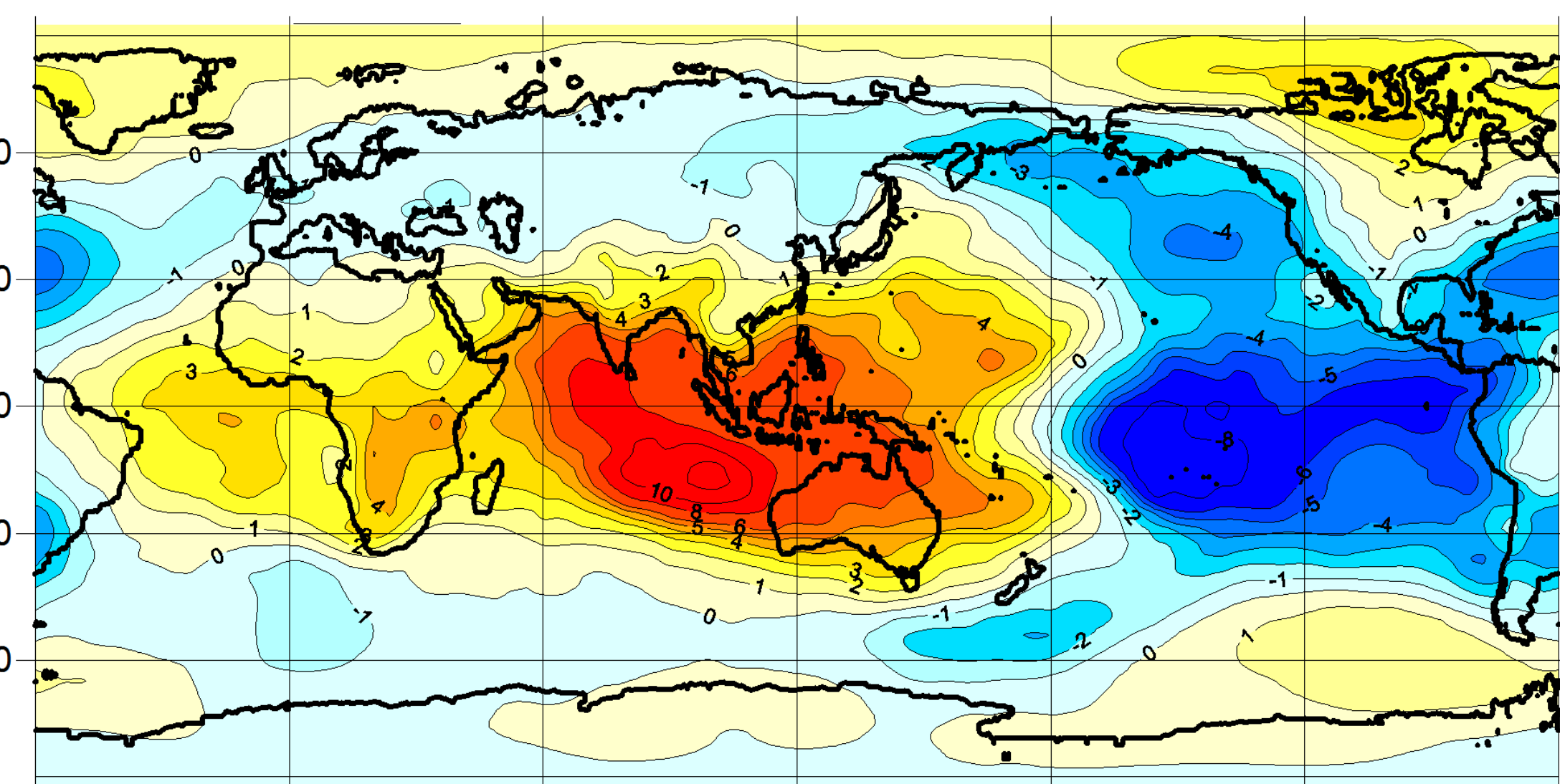
It is appropriate to mention also that the winter of 1997-98 accompanied by an enlargement of Barents Sea ice cover. Thus, a conclusion arises that detected disturbances of Barents Sea area environmental features in all likelihood connected with GAO generated anomalies.

Some Authors' Bibliography on the subject:

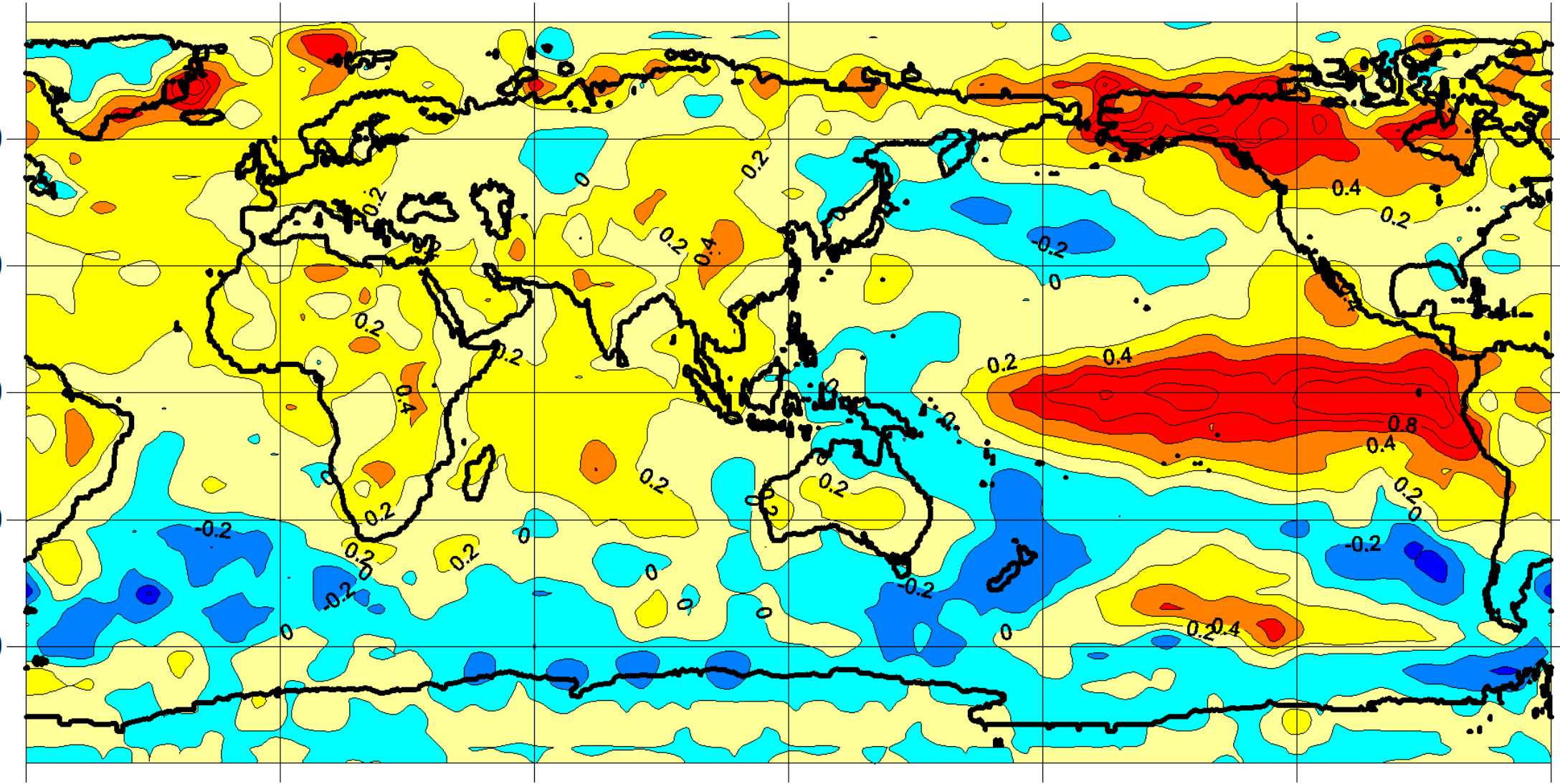
1. Sidorova A.N., Shcherbinin A.D. Barents Sea hydrodynamics change during the El Niño event. Doklady Earth Sciences. 01/2009; 429(2):1562-1566.
2. Sidorova A.N., Shcherbinin A.D. Hydrometeorological conditions in the Barents Sea during El Niño of 1997-1998. Russian Meteorology and Hydrology. 03/2011; 36(3):185-192.
3. Byshev V.I., Neiman V.G., Romanov Yu.A., Serykh I.V. El Niño as a Consequence of the Global Oscillation in the Dynamics of the Earth's Climate System. Doklady Earth Sciences. 2012. vol. 446, Part 1, pp. 1089-1094.



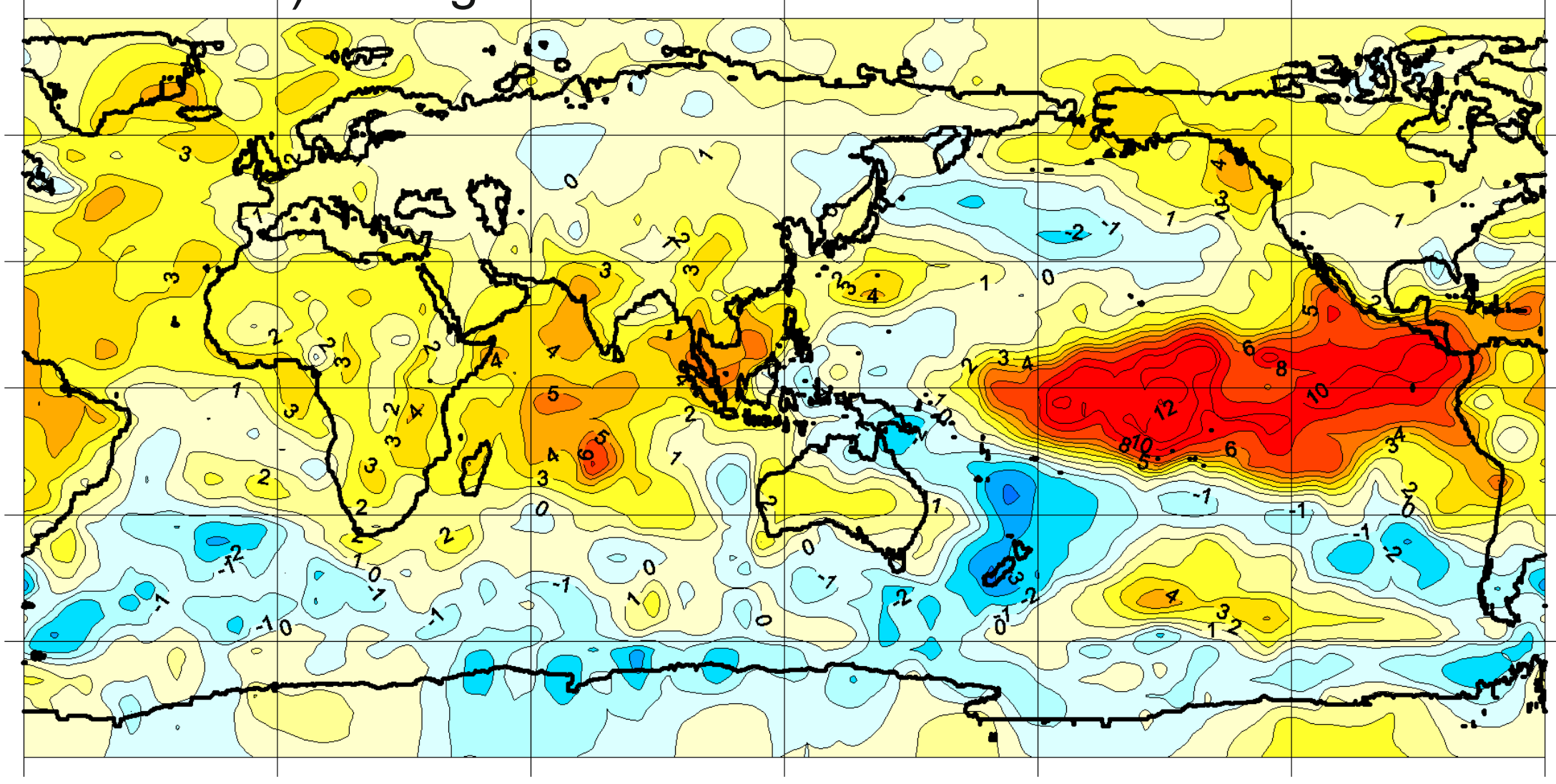
Anomalies of the sea-level atmospheric pressure and appropriated geostrophic wind (23 events of El Niño) averaged for 1920-2013.



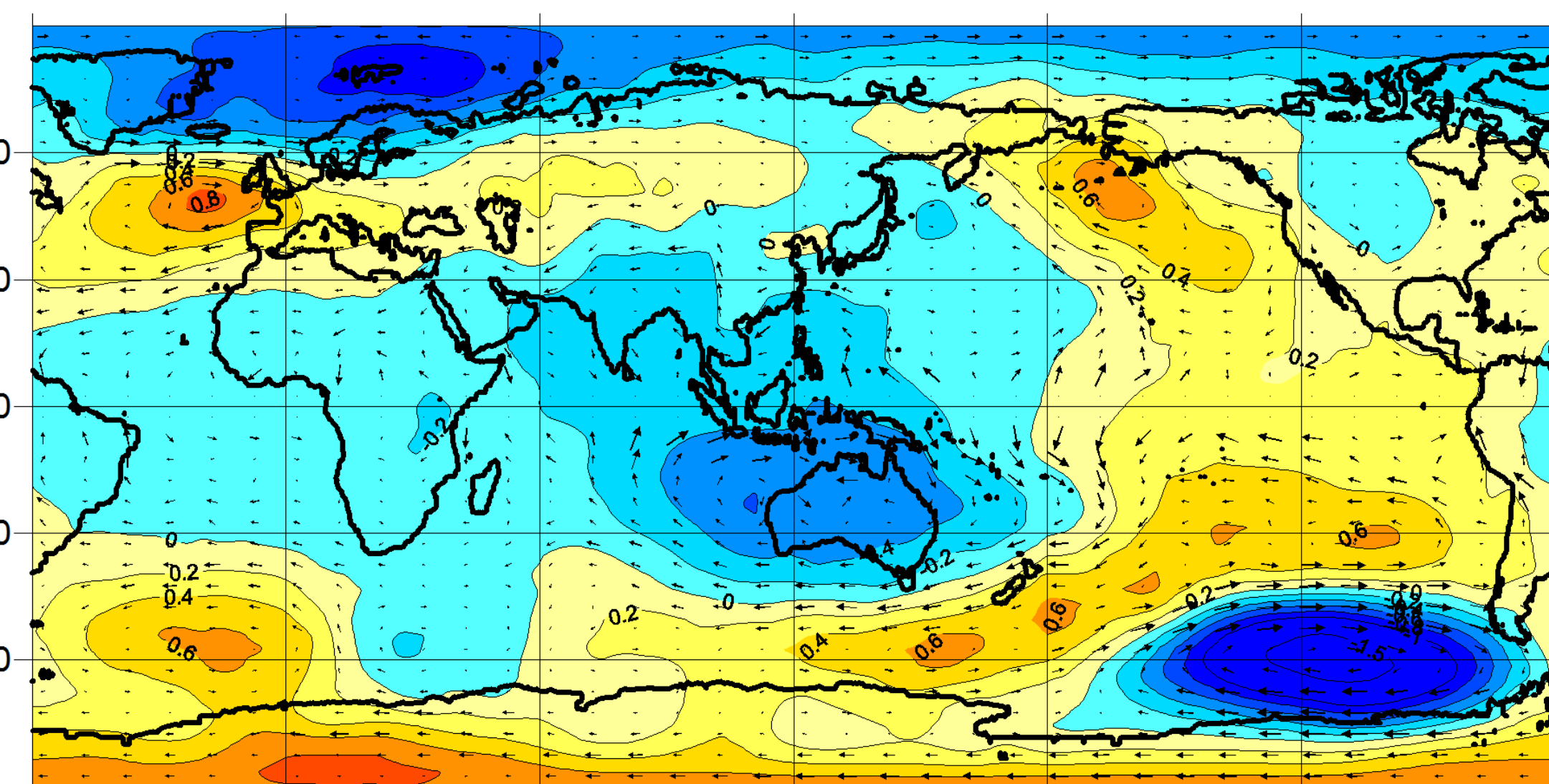
Student test of the anomalies of the sea-level atmospheric pressure (23 events of El Niño) averaged for 1920-2013.



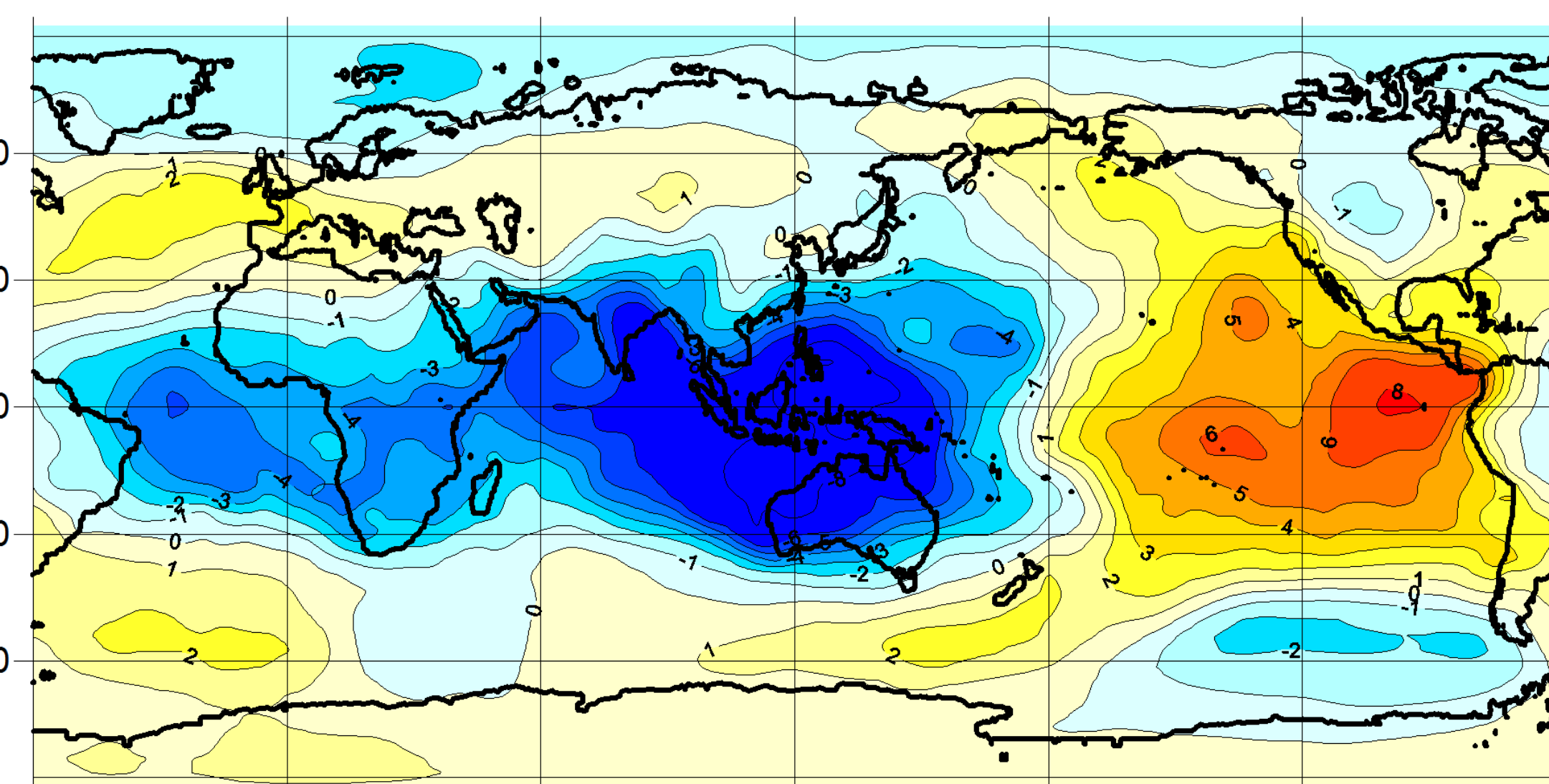
Anomalies of the near-surface temperature (23 events of El Niño) averaged for 1920-2013.



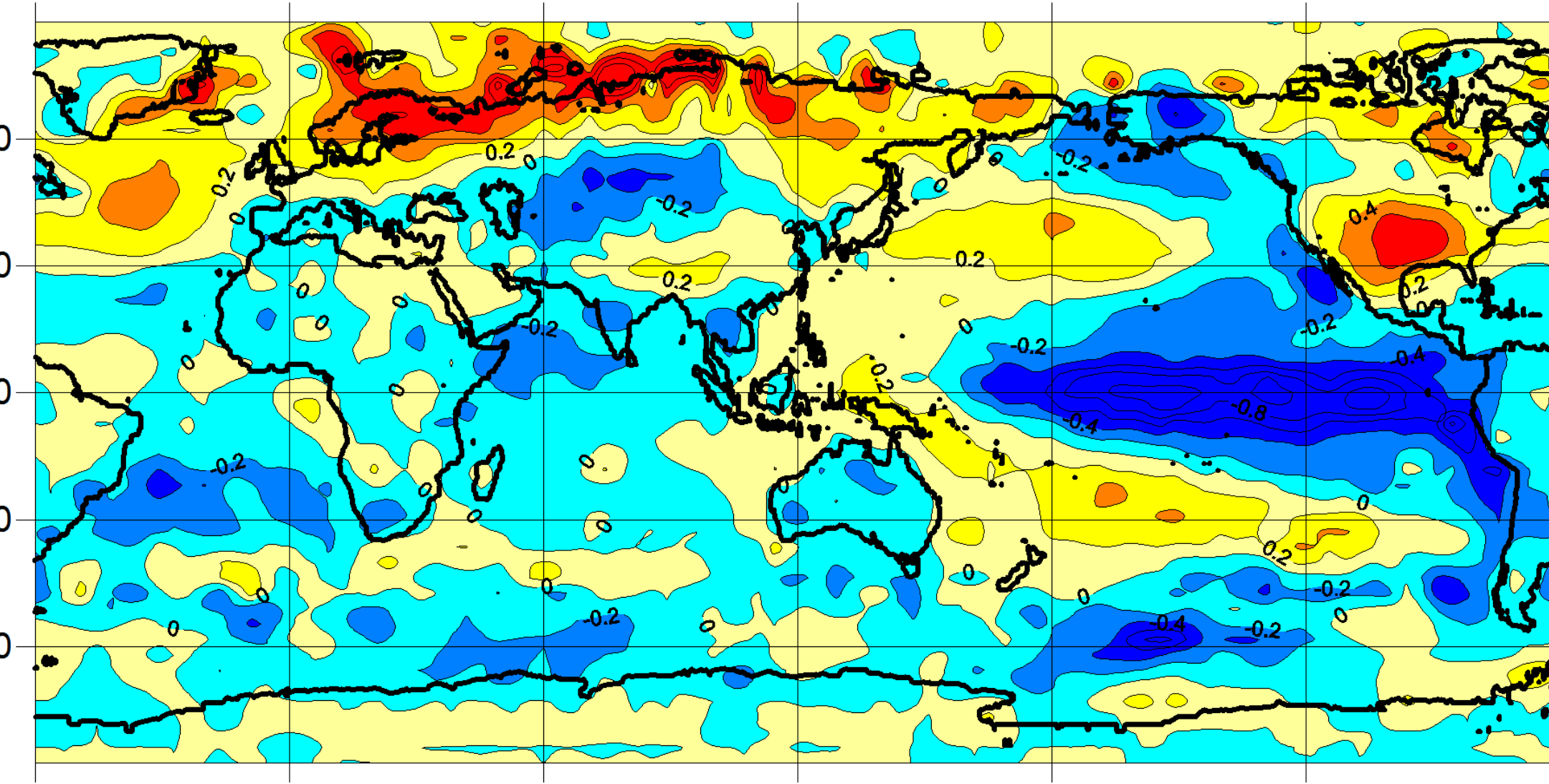
Student test of the anomalies of the near-surface temperature (23 events of El Niño) averaged for 1920-2013.



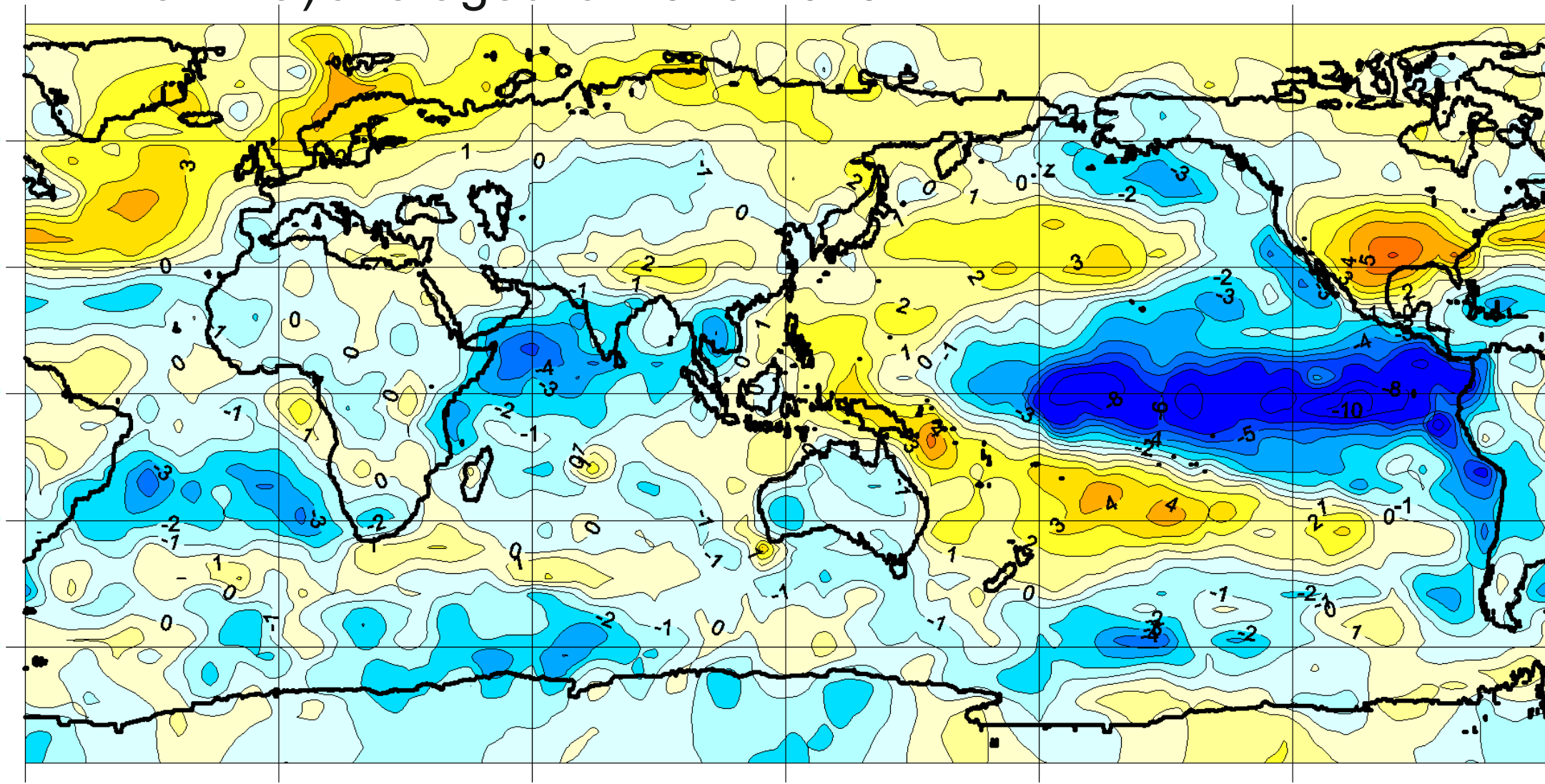
Anomalies of the sea-level atmospheric pressure and appropriated geostrophic wind (25 events of La Niña) averaged for 1920-2013.



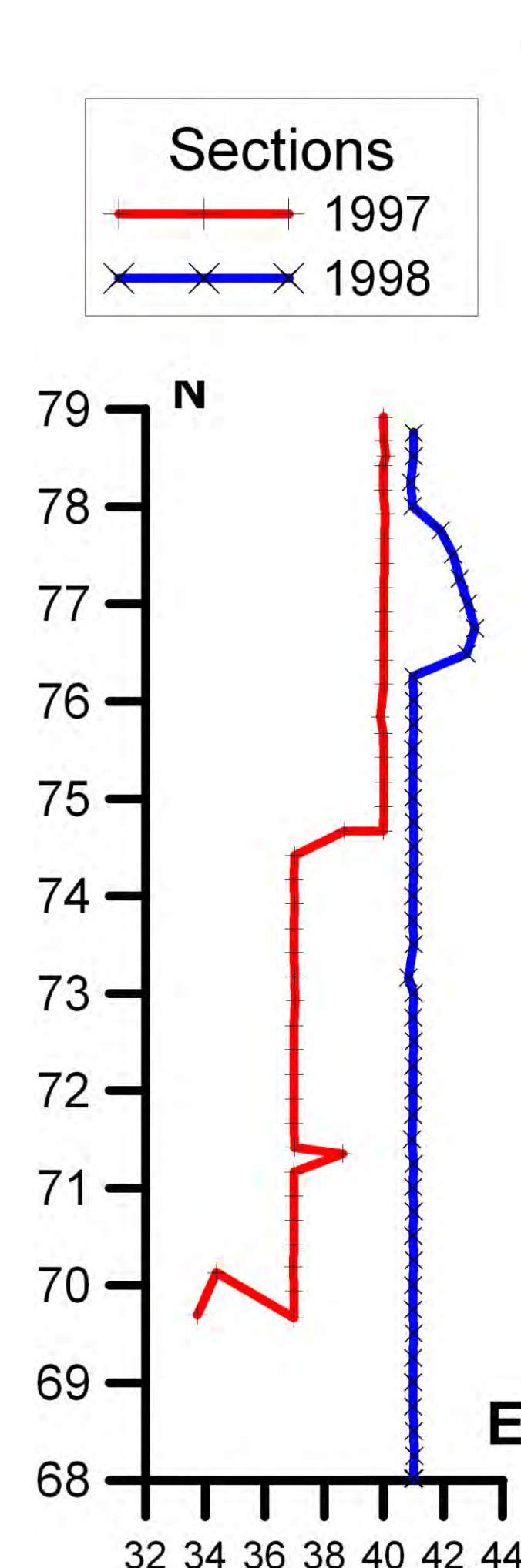
Student test of the anomalies of the sea-level atmospheric pressure (25 events of La Niña) averaged for 1920-2013.



Anomalies of the near-surface temperature (25 events of La Niña) averaged for 1920-2013.

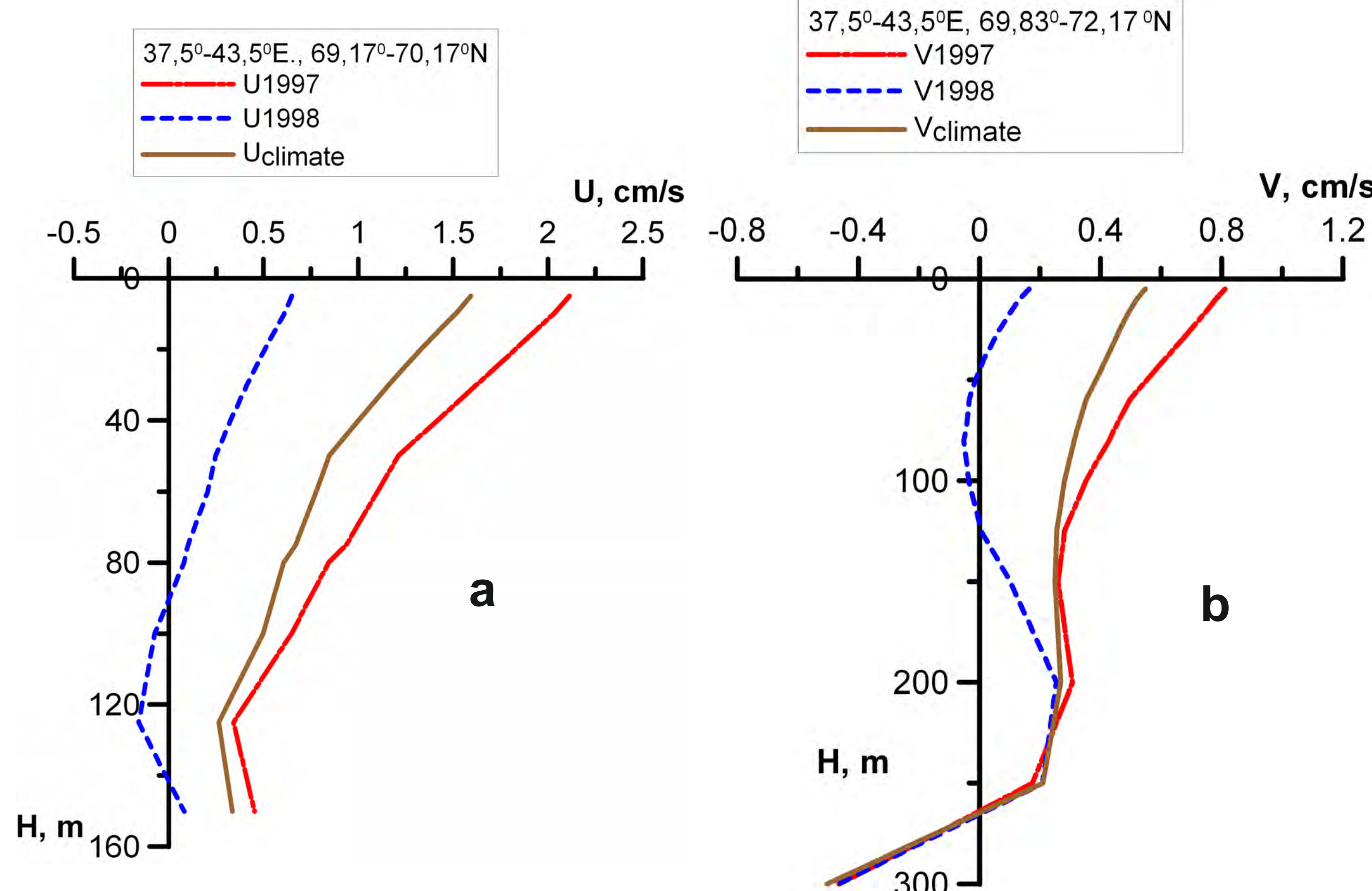


Student test of the anomalies of the near-surface temperature (25 events of La Niña) averaged for 1920-2013.



Hydrographic sections location

Meridional sections of the differences of temperature ($T=T_{1998}-T_{1997}$ ($^\circ\text{C}$)); and salinity ($S=S_{1998}-S_{1997}$ (o/oo)) along 41°E ; and meridional ($V=V_{1998}-V_{1997}$ (cm/s)) and zonal ($U=U_{1998}-U_{1997}$ (cm/s)) velocity components along 40.5°E . The areas of negative values are marked in blue.



Vertical distributions of the mean horizontal velocity components derived from adjustment calculation runs with climate data (brown solid line) and assimilation of temperature (T) and salinity (S) data from 1997 (red line) and 1998 (blue line) hydrographic sections: (a) zonal velocity component U averaged over the $37.5-43.5^\circ\text{E}$ and $69.17-70.17^\circ\text{N}$ region; (b) meridional velocity component V averaged over $37.5-43.5^\circ\text{E}$, $69.83-72.17^\circ\text{N}$ region.